THE ASTROPHYSICAL JOURNAL, 268:632–637, 1983 May 15

THE DISTRIBUTION OF IONIZED GAS IN THE NUCLEI OF SPIRAL GALAXIES[1]

WILLIAM C. KEEL[2]
Lick Observatory, Board of Studies in Astronomy and Astrophysics, University of California, Santa Cruz
Received 1982 September 17; accepted 1982 November 5

ABSTRACT

Narrow-band digital images have been obtained for a sample of spiral galaxies selected to contain low-ionization emission regions in their nuclei. The images have been processed to yield pure Hα + [N II] images. These show that the optically emitting gas is usually concentrated in a nearly spherical core of half-intensity diameter typically 200 pc, often surrounded by a disk, in the galactic plane, traceable over a 600–900 pc diameter. This gas disk is not present in several cases in which it is expected by comparison with others of similar luminosity in emission, showing that some morphological variety exists among these emission regions.

Subject headings: galaxies: nuclei — galaxies: structure — interstellar: matter

I. INTRODUCTION

This is the second in a series of papers describing the results of a study of the properties of low-ionization emission regions in the nuclei of spiral galaxies. The first paper (Keel 1983*a*) shows that such emission is present in every spiral in which nuclear star formation is not important. The third paper (Keel 1983*b*) interprets the emission spectra of these objects. This paper traces the distribution and extent of the optical line emission in the nuclei of a number of spirals which were spectroscopically selected to have low-ionization emission regions. While this does not comprise a complete sample, the whole observed range of emission-line luminosity and equivalent width was covered in the sample reported here.

The extent and distribution of the gas associated with a galactic nucleus can, in addition to reflecting the properties of the gas, serve as tracers of the total mass distribution and physical conditions in the nuclear region. These factors interact to such an extent that there is an ambiguity in interpretation, between the presence of gas and its visibility through ionization and excitation. The extremes are represented by photoionization by a single source, in which all the gas within some distance (analogous to the Strömgren radius) of it is visible through conversion of UV continuum radiation to optical line emission, and shock heating, in which only the gas cooling just behind each shock is visible.

Long-slit spectroscopy can add velocity information. Such information was the first obtained on the distribution of gas in galactic nuclei. A net outward gas flow was found in M31 by Münch (1960) and in NGC 253 by Ulrich (1978). The nuclear emission lines in M81 cover a region about 10″ in diameter and show radial-velocity variations suggesting net loss of gas from the nucleus (Goad 1974); M51 is still more complex, with a large region of peculiar excitation and complex velocity structure (Goad, de Veny, and Goad 1979; Rose and Searle 1982).

Further incentive to investigate the gas distributions came from the knowledge that the peculiar emission-line ratios in the nuclei extend over resolved areas. Aside from the cases mentioned above, some such instances were noted on long-slit spectra by Rubin, Ford, and Thonnard (1980). The emission regions in the type 2 Seyfert NGC 1068 are resolved into discrete clouds (Walker 1968*a*), and the inner region of M87 shows considerable structure in the emission lines (Walker and Hayes 1967; Arp 1967; Walker 1968*b*). Spectra of the inner disks of NGC 7331 and NGC 5005, away from the nuclei, were obtained in this study and showed that the emission in these galaxies was resolvable as a region about 20″ in diameter. Further observations of edgewise galaxies showed that [N II] is sometimes present near the nucleus but well out of the galactic plane. To investigate this, emission-line images of a selection of bright spirals were obtained. This technique has great potential for mapping emission features in a level of detail almost impossible to achieve by blind spectroscopy, as was well demonstrated by an image of M87 obtained by Ford and Butcher (1979) in comparison with the spectroscopic results referenced above. An easier, photographic demonstration of the potential of difference imaging was afforded by Lynds and Sandage's (1963) picture of the Hα filament system around M82.

[1] *Lick Observatory Bulletin*, No. 943.
[2] Visiting Astronomer, Kitt Peak National Observatory, which is operated by Association of Universities for Research in Astronomy under contract with the National Science Foundation.

II. OBSERVATIONS

To map the distribution of emission lines in many of these nuclei, images through interference filters on and off Hα + [N II] were obtained with the video camera on the 2.1 m telescope of Kitt Peak National Observatory in a run from 1981 December 18–23. The detector, described by Robinson *et al.* (1979), consists of a SIT tube behind an image intensifier. The tube is read into an accumulating memory every 1.6 s. A 256×256 pixel area is used, with a pixel size of 0".55 at this telescope, covering an area 140" square. The intensifier produces some pincushion distortion in the outer part of the field, giving shifts less than 2 pixels over 70% of the image. This does not affect any of the results here and has not been corrected because of the large amount of computing time this would require.

To isolate spectral regions of interest, a set of interference filters, covering the range of central wavelengths 6450–6738 Å with FWHM 60–70 Å, was used. Because of time restrictions, flat field exposures were obtained through only two or three of these each night. Tests showed that this was sufficient to correct for the wavelength dependence of each pixel's sensitivity, as this does not change appreciably over ~ 100 Å. On-line and off-line images were reduced with different flat fields in each case to maintain statistical independence. The basic reductions—dark-frame subtraction, flat field division and correction for illumination effects by use of blank-sky frames, and normalization—were done by the KPNO batch routine VIDCAM.

Further reduction of the images to give essentially pure emission-line images used the KPNO Interactive Picture-Processing System (IPPS). Each on-line image was shifted (via bicubic interpolation) to match the registration of the corresponding off-line image. The shifts were calculated by measuring the peak coordinates of the galactic nucleus or nearby stars in both images. The on-line image was then scaled to give the proper flux relative to the off-line image needed to match the emission equivalent widths measured on spectra already obtained, taken through the corresponding area around the nucleus and after allowance for the transfer function of each interference filter. This "self-calibration" procedure removes effects of different filter transmissions or passing clouds and in this study allowed imaging of weak emission regions contributing only a few per cent of the intensity in the on-line image. It works very well for the nuclei; there is no guarantee that it is as accurate in the outer regions of the galaxies, since a change in the stellar population could change both the equivalent widths of absorption lines in the filter bands (notably Hα and Ca I λλ 6450–6500) and the continuum slope between the filter bands. This point is more conceptual than practical in this work, with inconsequential results for these data.

Many of the continuum-subtracted images show a light patch somewhat off the galaxy. This results from a reflection of the nucleus off of the interference filters, which were used in a nearly plane-parallel beam. The reflections were usually stronger in the off-band filters, thus appearing as negative flux in the subtractions (light on these reproductions).

The sizes of star images in the video camera frames were measured in frames taken at frequent intervals, to evaluate the effects of seeing. For three of the five nights involved, the star images had FWHM of 1".5 or less.

In a few cases, spectrophotometry of points away from the nuclei was obtained to check the nature of the emission. These data were obtained with image-dissector scanner systems at the 1 m Nickel reflector of Lick Observatory or the 1.5 m reflector at Mount Lemmon.

III. RESULTS

Some possible results of this program could be anticipated. Models for the behavior of gas in spiral bulges, such as those of Faber and Gallagher (1976) or Bregman (1978), indicated that under most expected conditions gas should either blow out of the nucleus as a hot wind or sink to the immediate nuclear region. Only in the presence of a substantial contribution to the local potential from material other than bulge stars could significant gas exist cool enough to radiate optically at the distances from the nucleus considered here. The presence of such emission is clearly important in modeling the inner regions of these galaxies.

Specific structures might be expected in the line emission under some models. If shocks are the primary source of energy in the gas, large ones should be visible directly in many nuclei. The surface brightness in emission lines of typical nuclei suggested that only a few shocks are present along a given line of sight, being typically 4–6 times that predicted by the shock models of Shull and McKee (1979) for parameters known spectroscopically to be appropriate. There was no compelling reason to expect any particular spatial scale for the postulated shock fronts; the images might be expected to resolve them across the line of sight if they were very large and thus few in number. More generally, violent events in a nucleus might leave traces as filaments or other unusual and transient forms.

The results actually obtained showed a wide variety of forms and structures in the nuclear gas. Some appreciation of them may be gained from inspection of a number of video camera frames. Descriptions of these and various special features they exhibit follow. Each image is a Dicomed reproduction produced by the KPNO IPPS. The gray scale is linear in intensity and was adjusted in both zero point and slope before output to emphasize the brightness range of greatest interest.

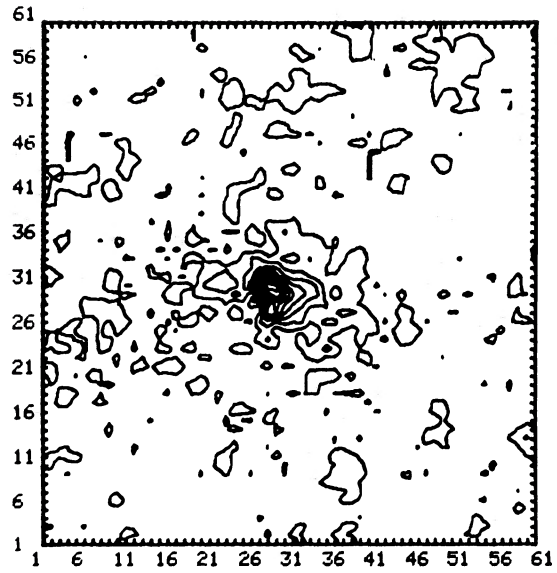

FIG. 2.—Contour display of the inner part of the Hα+[N II] image of NGC 7331. The contour interval is 10% of the peak. Each tick mark is one pixel or 0.″55.

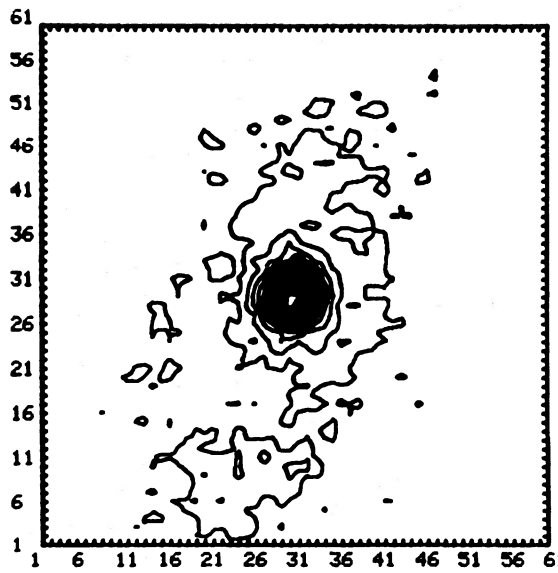

FIG. 5.—Contour display of the Hα+[N II] image of NGC 4579. The contour interval is 7% of peak; scale and orientation as in Fig. 2.

Galaxies with nuclear disks of emission are shown first. NGC 7331 (Fig. 1 [Pl. 10]) is a typical, well-observed case. The emission-only image shows a concentration at the nucleus, surrounded by a structure elongated in the same direction as the galaxy image. It can be traced above the noise, to about 10% of the peak level, over an extent of 20″ or 1.5 kpc. Spectroscopy with an 8.″1 aperture measured [N II] at positions centered 10″ north and south, 10″ east, and 18″ south, confirming that the emission spectrum in the extended region has characteristics similar to that in the nucleus. A contour plot of the inner portion of the line-only image (Fig. 2), with its outermost contour at the 10% level, shows the elongation well, and also shows that most of the emission comes from a region only 4″ in diameter (FWHM). This combination of a small central concentration and extended structure aligned with the galactic disk is common among these galaxies. These images also afford a graphic demonstration of the low emission-line luminosities in many nuclei—a number of much brighter H II regions appear, especially in NGC 7331 and NGC 772.

Similar morphology is seen in NGC 3169. The image including Hα+[N II] is shown before and after continuum subtraction in Figure 3 (Plate 11). The morphology of the galaxy as a whole is somewhat disturbed, perhaps as a result of interaction with NGC 3166 (cf. the classification "tides" in Sandage and Tammann 1981, hereafter RSA), but the inner region shown in these images is quite regular.

NGC 4579 shows a similar but more structured emission morphology (Fig. 4 [Pl. 12]). There is evidence of a weak spiral pattern or absorbing lane to the northeast of the nucleus. A spectrum of the brightest emission in this region confirms that it has approximately the line ratios of the nucleus, in the red. A contour plot of this image appears as Figure 5.

Several galaxies highly inclined to the line of sight were observed to study the z-extent of emission. NGC 4216, NGC 5005, and NGC 4192 (Fig. 6 [Pl. 13]) are all such galaxies, with inclinations of 78°, 63°, and 74°, respectively, based on axial ratios in de Vaucouleurs, de Vaucouleurs, and Corwin (1976, hereafter RC2) and on the transformation in Krumm and Salpeter (1979). All show that the nuclear emission at low levels is greatly elongated in the galactic plane; for this reason, such a structure may be called a disk. The emission near the nucleus of NGC 5005 is similar to that at the nucleus, but with narrower lines. The prominent patch of emission southeast of the nucleus of NGC 4192 is an H II region, as shown by spectra from Mount Lemmon.

A range of scales exists for the nuclear disks. Two galaxies with less prominent, but detected, disk structures around the nuclear concentrations are the Sab NGC 3368 (Fig. 6) and the Sb NGC 4501 (Fig. 7 [Pl. 14]). These seem intermediate between the extensive disks above and those objects (below) with very weak or undetected extended structures.

Two spirals of very great linear extent were observed, to see whether the nuclear gas distributions scale with

the galaxy in extreme cases. NGC 3312, a member of the Hydra I (Abell 1060) cluster, can be traced photographically to a diameter of 55 kpc ($H_0 = 75$ km s^{-1} Mpc^{-1}). UGC 2885 is the largest known spiral, with a Holmberg diameter of 230 kpc (Rubin, Ford, and Thonnard 1980). Nuclear gas disks appear at large linear sizes in these objects. In both NGC 3312 and UGC 2885 (Fig. 8 [Pl. 15]), the structures are of larger extent than in the other galaxies studied. The diameters measured, to the usual 10% level, are 2.4 kpc for NGC 3312 and 2.2 kpc for UGC 2885; this value is somewhat affected by galactic obscuration and is in fact likely larger. UGC 2885 appears at the lower left of the image; this kept a bright star out of the instrument's field of view. The white spot near it is a stellar reflection.

A small nuclear emission patch is seen in M94 = NGC 4736 (Fig. 7). The spectacular ring of H II regions seen in this image coincides with an abrupt drop in disk surface brightness. The radio continuum morphology, roughly the same as that in Hα, prompted Sanders and Bania (1976) to suggest that a violent event in the nucleus had left a compression wave traveling outward through the disk, inducing star formation at the current position of the ring.

At the other extreme are nuclei in which no emission beyond a small knot at the nucleus was seen. In several of these, the emission luminosity and contrast are high enough that such a structure would be detected if present to a degree like that in the first galaxies mentioned (NGC 7331, 3169, 4579). The luminosity distributions of resolved and unresolved emission (Fig. 9) show that, while simple scaling may make disks undetectable in weak-emission objects, luminosity is not the sole factor in visibility of a gas disk. There is a real morphological difference. Examples of nuclei with only concentrated emission seen are NGC 3521, NGC 3338, and NGC 772 (Fig. 10 [Pl. 16]). The nucleus in NGC 3338 is very faint in emission.

Some galaxies have structure not well described by the sequence of changing importance of a kiloparsec-scale disk and the nucleus inferred from the galaxies above. NGC 2841 (Fig. 11) shows an apparent one-sided bar in emission. It is not clear whether this is continuous or the result of a single patch of emission near the nucleus. NGC 488 is a similar case, in which a galaxy with no evidence of a stellar bar has the appearance of a bar in the emission-line images.

Very complex emission structure, involving numerous H II regions as well as an irregular nuclear low-ionization zone, appears in the "Black-Eye" galaxy, NGC 4826 (Fig. 11 [Pl. 17]). Some of the gaps in the emission reflect dark absorbing lanes; the synthetic population (Paper III) indicates a bulk reddening of $E_{B-V} = 0.30$ for the nucleus. The gas distribution in NGC 4438 (Fig. 11) is unusual in being elongated perpendicular to the isophotes of the galaxy. This galaxy is of ambiguous

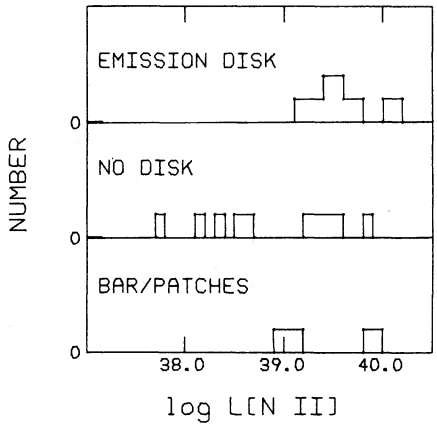

FIG. 9.—Luminosity distribution of various morphological kinds of nuclear low-ionization emission regions. The emission luminosity is given as that in [N II] λ6584, because of large uncertainties in the absorption correction for weak Hα.

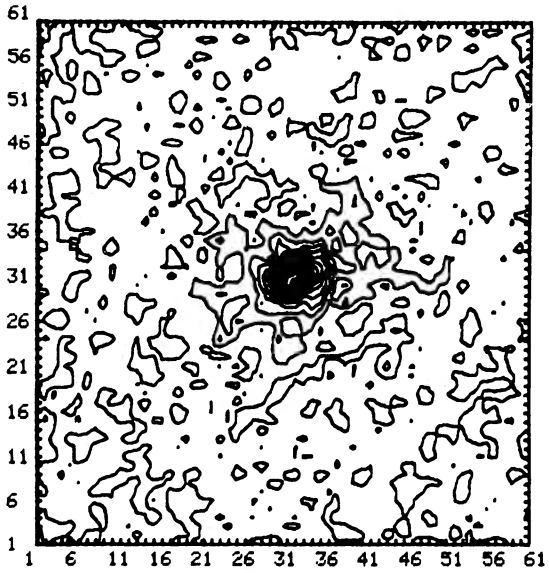

FIG. 13.—Contour display of the Hα+[N II] image of NGC 7217. The contour interval is 7% of peak.

classification due to strong interaction with NGC 4435, with classifications ranging from S0 pec in the RC2 to Sb (tides) in the RSA. The radial velocity of NGC 4438 allowed use of filter combinations which isolated [N II] and Hα from one another; their distributions in the nucleus are the same, as is the case in all the other galaxies for which such data were obtained (NGC 4826, 488, 772, 3623, 3627, and 7479). A final point of interest is that the most intense emission, though not the fainter "fan" to the southeast, follows essentially the 6 cm

TABLE 1

MORPHOLOGY OF LOW-IONIZATION EMISSION REGIONS

Galaxy	Type	Disk?	Extent (arcsec)	Major FWHM (arcsec)	Orientation (degrees)
N0157	Sc	no	...	3	...
N0488	Sab	bar	8	2.5	45
N0772	Sb	no	...	4	...
N1097[a] ...	SBbc	no	...	2	...
N2639	Sa	possible	10	4	145
N2683	Sb	no	...	5	...
N2841[b] ...	Sb	bar	10	3.5	105
N3031	Sb	yes	35	8	165
N3169	Sb	yes	16	5.5	60
N3190	Sa	yes	12	3.5	150
N3312	Sab	yes	15	3	5
N3338	Sbc	no	...	2.5	...
N3368	Sab	possible	10	2	165
N3521	Sb	no	...	3	...
N3623	Sa	no	...	2.7	...
N3627	Sb	bar	22	5	150
N3884	Sab	bar	9	3	85
N4192	Sb	yes	15	3	135
N4216	Sb	yes	20	8	25
N4419	SBab	no	...	5	...
N4438	Sb p	see text	8	3	120
N4450	Sab	no	...	3	...
N4501	Sbc	no	...	3	...
N4565	Sb	possible	8	3	130
N4579	Sab	yes	35	5	70
N4594	Sab	yes	15	3	85
N4736	Sab	yes	8	3.5	70
N4826	Sab	patchy	30	8	120
N5005	Sb	yes	16	4	75
N5033	Sbc	yes	70	4	165
N7177	Sab	no	...	3	...
N7217	Sb	yes	30	4.5	90
N7331	Sb	yes	21	4	165
N7479	SBbc	bar	13	3.5	5
U2885	Sc	yes	6	3	55

NOTE.—Orientations are north through east. FWHM is corrected for seeing effects.
[a]H II ring.
[b]Not along disk.

continuum map (van der Hulst, Crane, and Keel 1981). The peculiar structure of this nucleus is undoubtedly strongly influenced by the galaxy interaction.

The best evidence for small-scale spatial structure in the emission lines is seen in an image of NGC 7217 (Fig. 12 [Pl. 18]) taken in excellent seeing. Several filamentary structures appear; examination of count rates and images of other objects of similar surface brightness suggests that at least some of these are real. Several can be identified in a contour plot (Fig. 13). Such features were a primary goal of the program, since they might represent gross irregularities in the gas distribution or its ionization (e.g., shock fronts). Further interpretation must await confirmation and spectroscopy of the apparent filaments.

Altogether 39 galaxies were imaged in Hα+[N II]. The emission morphologies are summarized in Table 1. The maximum size listed is the longest dimension of detected nuclear emission, at roughly 10% of typical peak intensity or a surface brightness in Hα+[N II] of 2.2×10^{-16} ergs cm^{-2} arcsec^{-2} s^{-1}. There is no distinction in Hubble type between galaxies with resolved extended emission and those with only a small core observed.

The listed FWHM for nuclear emission has been corrected for the seeing profile as evaluated in star images, under the assumption that both intensity distributions are Gaussian. The seeing was generally good enough that diameters of 3″ and greater are clearly resolved. The inner portion of the ionized region appears round in most of these galaxies; the seeing measurements (typically 1″.5 FWHM) indicate that this is not predominantly a seeing effect, though a small degree of rounding of the isophotes has taken place.

IV. DISCUSSION

Several characteristics of the nuclear emission and the nuclei themselves may be inferred from these observations. The emission is often smoothly distributed, so it does not arise in a small number of discrete areas; this means that, for example, young supernova remnants (SNR) do not contribute significantly to the total emission. This is supported by the invisibility of any remnant of SN 1959 in NGC 7331 on the [N II]+Hα image, though the line luminosity grows with time at this stage as matter is swept up and shocked. The same general argument applies to other energetic stellar objects, such as binary X-ray sources. Quantitative limits are difficult to set without a specific model to test against; in most cases the line emission does not come from a few (< 10) point sources in the inner emitting region. This does not necessarily apply to the ionizing sources, since an energetic point source could be quite capable of ionizing the whole nuclear gas content (as in luminous active nuclei).

Limits may be set on the importance of winds in sweeping gas from the bulges of spirals. It is clear from the occurrence of emission lines (Paper I) that some gas always remains at the nucleus; spiral bulges are not completely swept, as some ellipticals are (Faber and Gallagher 1976). The emission seen away from the center implies the presence of relatively cool gas in a region which, in many wind models, would be occupied only by a hot wind, whose detection is essentially impossible with present techniques (Mathews and Baker 1971). This is slightly surprising, since if any part of a disk galaxy can sustain a wind, it is the bulge (Bregman 1978); an additional mass component seems the most obvious way to stabilize the gas. This might take the form of an inner disk or a massive "halo" within the bulge (Bregman 1978). A role for bulge winds is suggested by the fact that the observed emission lines imply gas masses much smaller than expected for accumulated mass lost from stars over a large fraction of the Hubble time, no matter what details of its ionization are assumed. This point will be discussed further in Paper III.

A final remark on distributions of gas in spiral bulges is that the distributions seem to follow the starlight in outline, if not details of radial distribution. This supports an internal origin for the gas, rather than recent infall from outside the galaxies. Infall, to be important, must have occurred long enough ago that the gas has assumed the galaxy's plane of rotation in those cases in which a disk of gas is seen. The extent to which the emission and continuum isophotes follow one another indicates that the gas and stars are closely related dynamically in the innermost parts of most of these galaxies, supporting the view that most of the gas originated in the stars or that it has been in the nucleus long enough to have adopted the local dynamical properties.

V. SUMMARY

Emission-only images of the nuclei of 39 spiral galaxies with low-ionization emission have been obtained. They show a typical gas structure consisting of a round core surrounded by a disk, in the same plane as that of the galaxy. Some differences are seen among galaxies; some lack the disk of emission, and several cases show complex structure due to interactions or nearby star formation. A few nuclei show evidence of fine structure on scales of a few tens of parsecs.

The observations at Kitt Peak were very materially assisted by several of the staff there, particularly Suzanne Hammond and George Will. Operation of the IDS spectrograph at Mount Lemmon is supported by the NSF through a grant to UC, San Diego. The NSF also supported me through a graduate fellowship during a portion of this work, and under grant AST 80-19322 during the remainder.

REFERENCES

Arp, H. C. 1967, *Ap. Letters*, **1**, 1.
Bregman, J. N. 1978, *Ap. J.*, **224**, 768.
de Vaucouleurs, G., de Vaucouleurs, A., and Corwin, H. 1976, *Second Reference Catalog of Bright Galaxies* (Austin: University of Texas Press) (RC2).
Faber, S. M., and Gallagher, J. S. 1976, *Ap. J.*, **204**, 365.
Ford, H. C., and Butcher, H. R. 1979, *Ap. J. Suppl.*, **41**, 147.
Goad, J. W. 1974, *Ap. J.*, **192**, 311.
Goad, J. W., de Veny, J. B., and Goad, L. E. 1979, *Ap. J. Suppl.*, **39**, 439.
Keel, W. C. 1983*a*, *Ap. J. Suppl.*, in press (Paper I).
_____. 1983*b*, *Ap. J.*, in press (Paper III).
Krumm, N., and Salpeter, E. E. 1979, *Ap. J.*, **228**, 64.
Lynds, C. R., and Sandage, A. R. 1963, *Ap. J.*, **137**, 1005.
Mathews, W. G., and Baker, J. C. 1971, *Ap. J.*, **170**, 241.
Münch, G. 1961, *Ap. J.*, **131**, 250.
Robinson, W., Ball, W., Vokac, P., Piegorsch, W., and Reed, R. 1979, *Proc. Soc. Photo-Opt. Eng.–Instr. Astr.*, **III**, 98.
Rose, J. A., and Searle, L. 1982, *Ap. J.*, **253**, 556.
Rubin, V. C., Ford, W. K., Jr., and Thonnard, N. 1980, *Ap. J.*, **238**, 471.
Sandage, A., and Tammann, G. A. 1981, *A Revised Shapley-Ames Catalog of Bright Galaxies* (Washington: Carnegie Institution) (RSA).
Sanders, R. H., and Bania, T. M. 1976, *Ap. J.*, **204**, 331.
Shull, J. M., and McKee, C. F. 1979, *Ap. J.*, **227**, 131.
Ulrich, M.-H. 1978, *Ap. J.*, **219**, 424.
van der Hulst, J. M., Crane, P. C., and Keel, W. C. 1981, *A.J.*, **86**, 1175.
Walker, M. F. 1968*a*, in *IAU Symposium 29, Nonstable Phenomena in Galaxies*, ed. M. Arekeljan (Yerevan: Armenian Academy of Sciences), p. 21.
_____. 1968*b*, *Ap. Letters*, **2**, 65.
Walker, M. F., and Hayes, S. 1967, *Ap. J.*, **149**, 481.

WILLIAM C. KEEL: Kitt Peak National Observatory, P.O. Box 26732, Tucson, AZ 85726

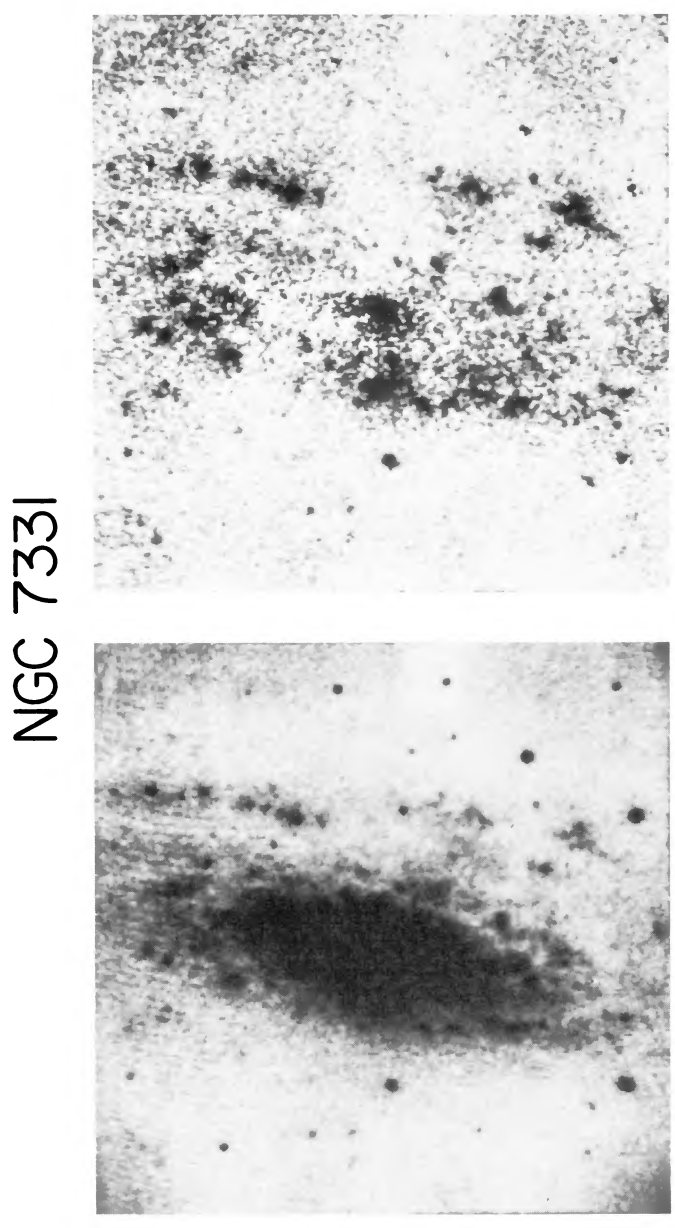

FIG. 1.—Image of NGC 7331 centered at 6583 Å, before and after subtraction of an image in the pure stellar continuum at 6450 Å. The field is 140″ square; north is at the top.

KEEL (*see* page 634)

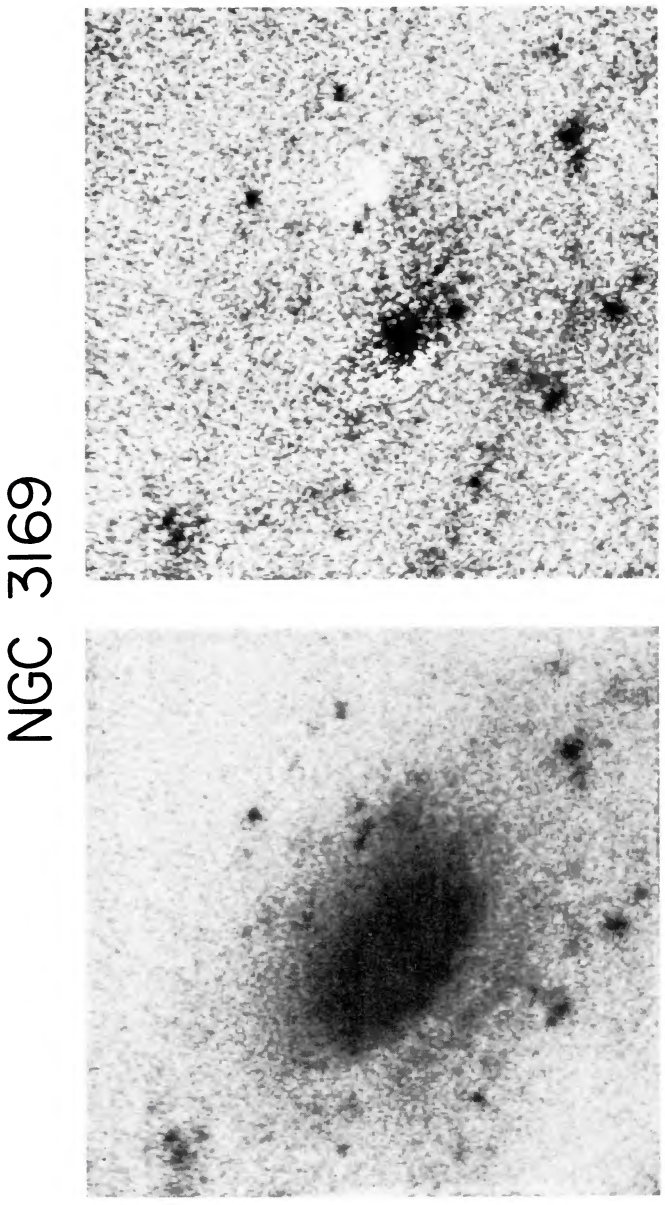

FIG. 3.—Observed and continuum-subtracted versions of the 6607 Å image of NGC 3169

KEEL (*see* page 634)

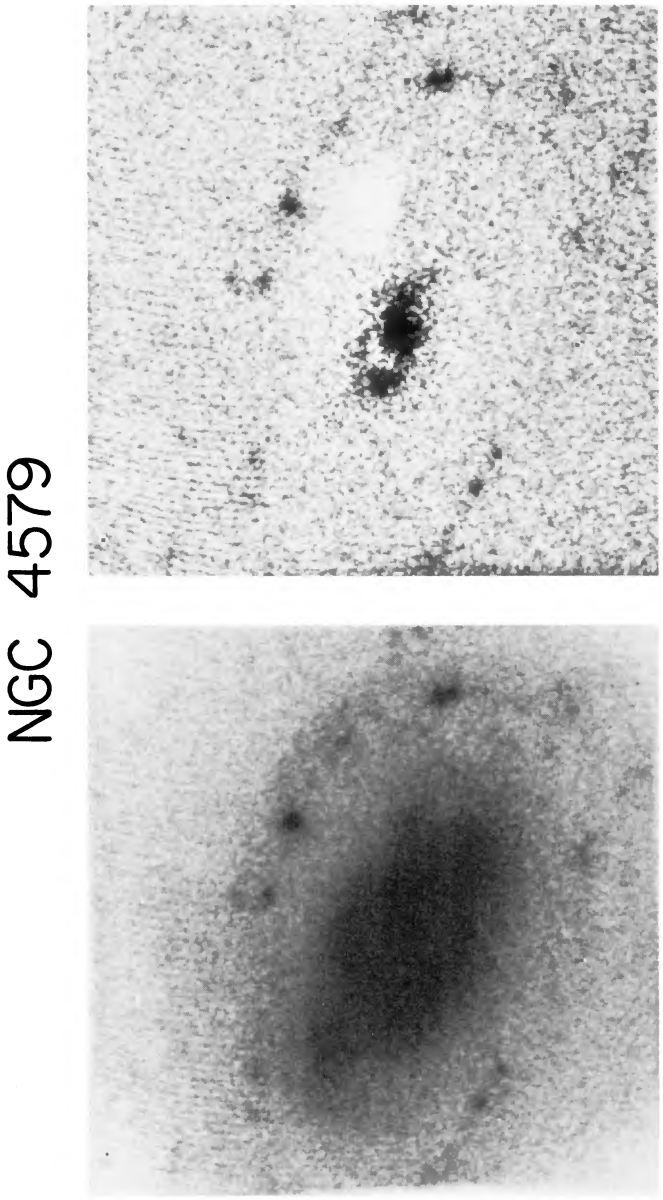

FIG. 4.—Observed and continuum-subtracted versions of the 6607 Å image of NGC 4579

KEEL (*see* page 634)

PLATE 13

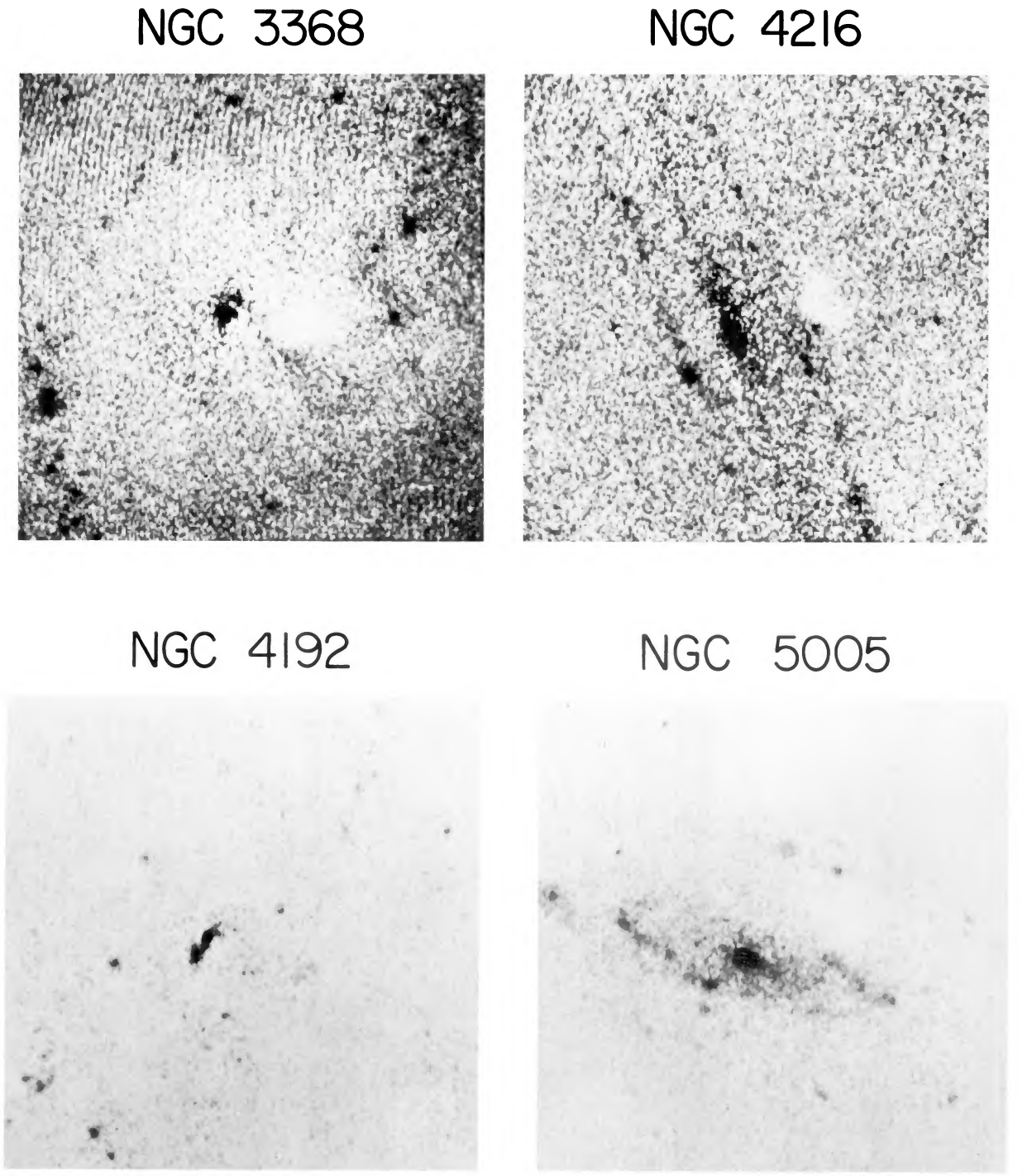

FIG. 6.—Continuum-subtracted images in Hα + [N II] of spirals with nuclear emission disks: (*top*) NGC 3368 and 4216, (*bottom*) NGC 4192 and 5005. All images are 140″ square with north at the top.

KEEL (*see* page 634)

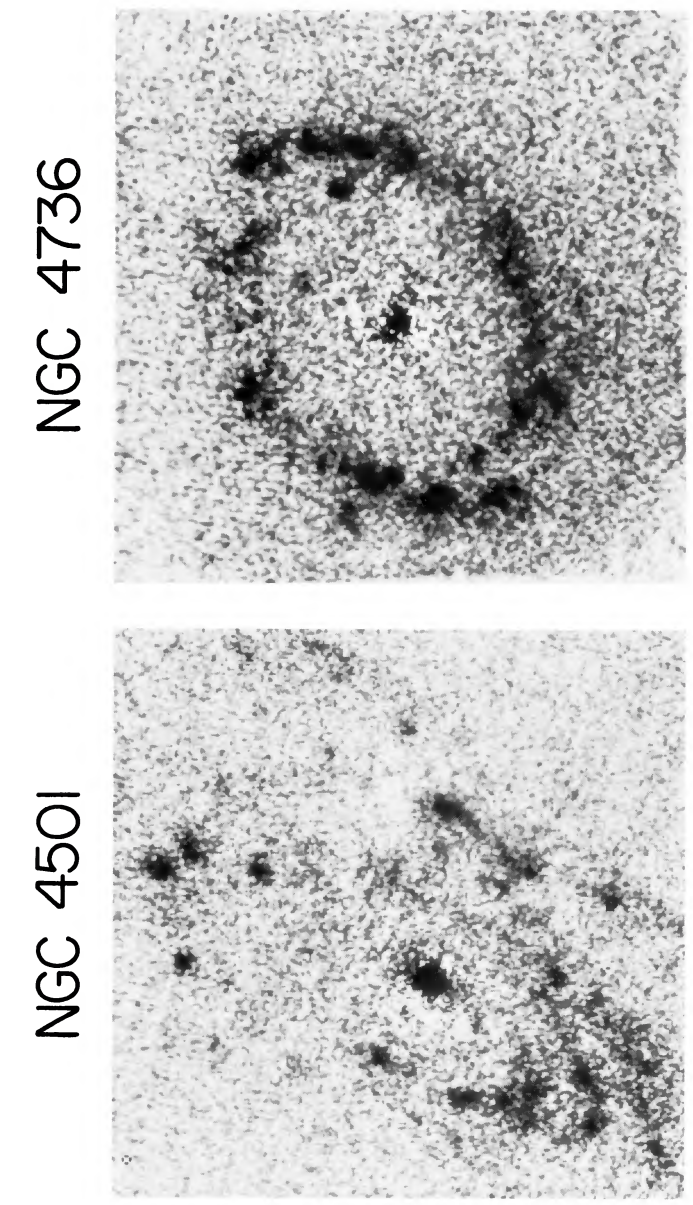

FIG. 7.—Images in Hα + [N II] of galaxies with small nuclear emission disks: NGC 4501 and 4736

KEEL (*see* page 634)

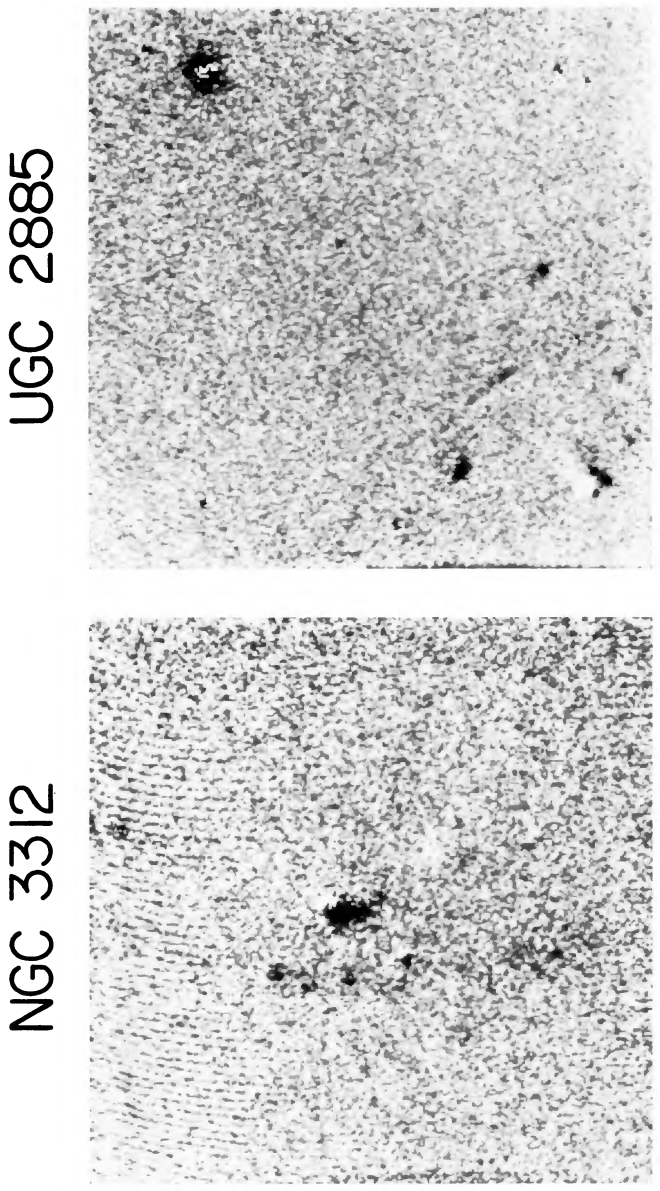

FIG. 8.—Images in Hα + [N II] of two giant spirals: NGC 3312 and UGC 2885

KEEL (*see* page 635)

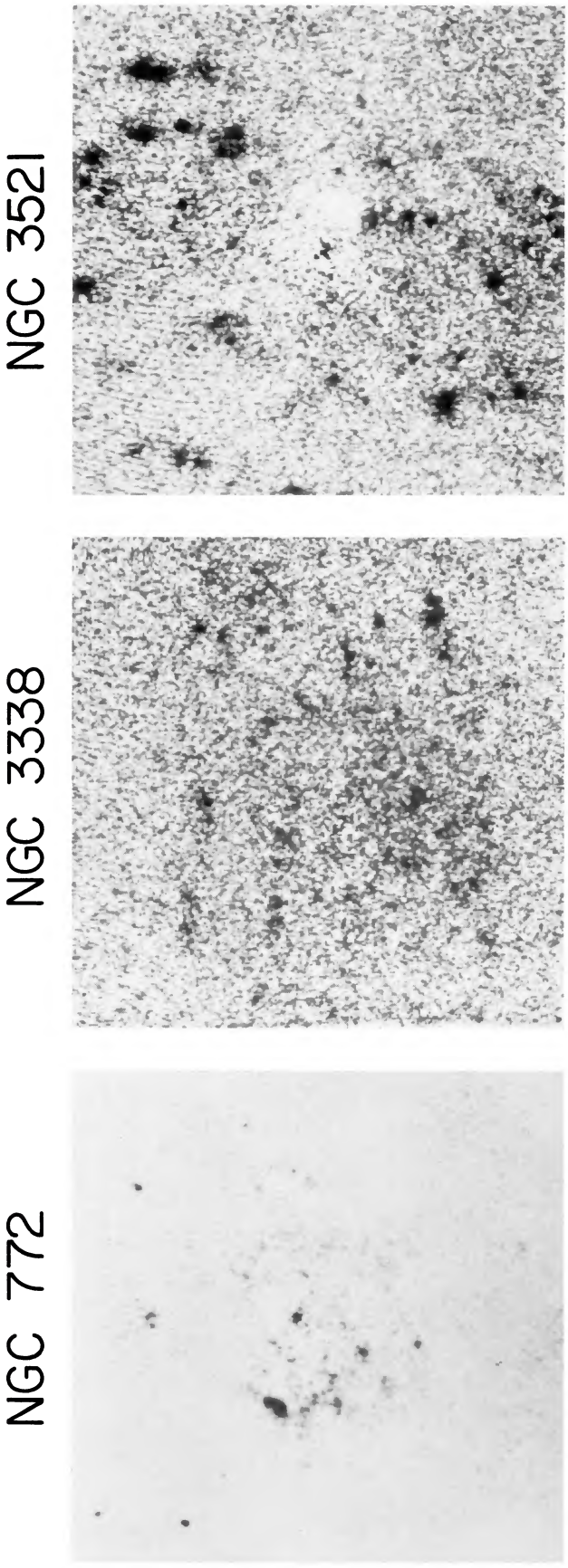

FIG. 10.—Images in Hα +[N II] of galaxies without detected nuclear emission disks: NGC 772, 3338, and 3521

KEEL (*see* page 635)

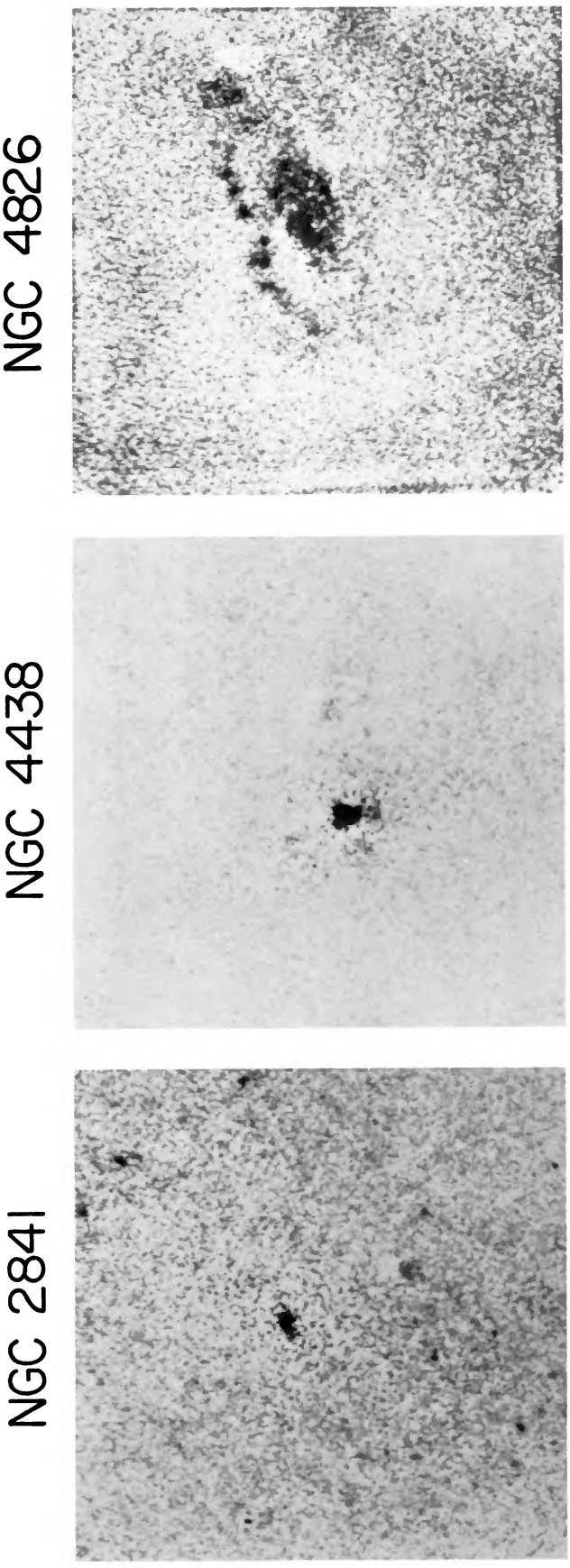

FIG. 11.—Images in Hα + [N II] of galaxies with complex nuclear emission structures: NGC 2841, 4826, and 4438

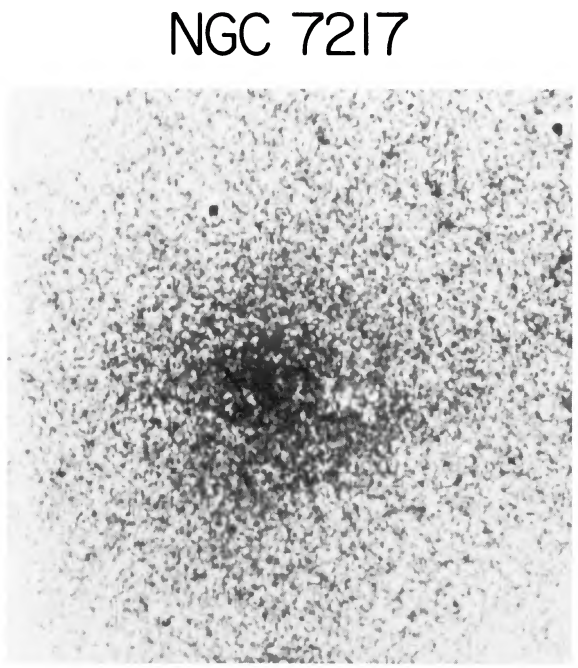

FIG. 12.—Emission-only image of NGC 7217 in Hα + [N II]. Note the apparent filamentary structure.

KEEL (*see* page 636)